A Magnetic Post Approach for Measuring the Viscoelasticity of Biomaterials

Kevin S. Bielawski and Nathan J. Sniadecki

***Abstract*— A wide variety of tools are used in studying the viscoelasticity of materials. Devices used range from microbeads dispersed in a fluid to standard cone-and-plate rheometers. In order to further the techniques for *in situ* testing of materials, we have developed a new microdevice for measuring viscoelasticity. The device uses a polydimethylsiloxane post filled with magnetic microparticles. The force on the post is controlled with oscillating magnetic fields in order to measure properties of a fluid or gel. The device was calibrated with mixtures of glycerol and then used to observe the gelation process for collagen gels. The results from using the new device had good agreement with previous experimental results. [2015-0197]**

***Index Terms*— Magnetic devices, magnetic materials, microelectromechanical devices, image analysis, biological materials.**

I. Introduction

RHEOLOGY is a field that studies viscoelastic nature of materials and how they behave when exposed to different conditions. There are a variety of devices used for measuring rheological properties on the microscale, including magnetic beads [1], atomic force microscopy (AFM) [2], magnetic AFM [3], and embedded magnetic wires [4]. Although these devices have been useful for studying fluid rheology, new tools are continuing to be developed for application-specific endeavors [5]–[7]. Some of the goals of new devices are to study small volumes of fluid and to perform *in situ* measurements.

Measurements of rheology are performed by shearing a fluid by moving two components of a system in relation to each other. A common rheology tool is a cone and plate rheometer that rotates a cone to shear a fluid [8]. One method to move components is through the use of soft polymeric structures, such as polydimethylsiloxane (PDMS), embedded with magnetic material. Several devices using mixtures of magnetic beads and PDMS have been built for applications including agitating fluids through either the use of biomimetic cilia [9], [10], or as larger flaps used to disrupt the fluid [11]–[13]. Magnetic microposts have also been used to pull on cells [14], and to act as actuators in a variety of configurations [15]–[17].

Manuscript received July 10, 2015; revised November 9, 2015; accepted November 22, 2015. This work was supported by the National Science Foundation through the Division of Civil, Mechanical, and Manufacturing Innovation under Grant 1402673. Subject Editor S. Konishi.

K. S. Bielawski is with the Mechanical Engineering Department, University of Washington, Seattle, WA 98195 USA (e-mail: ksbielaw@uw.edu).

N. J. Sniadecki is with the Mechanical Engineering Department and the Department of Bioengineering, University of Washington, Seattle, WA 98195 USA (e-mail: nsniadec@uw.edu).

Color versions of one or more of the figures in this paper are available online at http://ieeexplore.ieee.org.

Digital Object Identifier 10.1109/JMEMS.2015.2504844

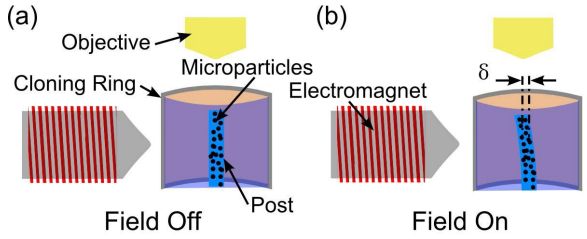

Fig. 1. Overview of the post with the magnetic field (a) off and (b) on. A PDMS post with embedded magnetic particles is adhered to the bottom of a well and deflects under the presence of a magnetic field. The deflection of the top of the post, δ, is measured with an optical microscope.

In this paper, we describe a new device which combines magnetic microposts and rheological devices in order to make a magnetically actuated tool which is capable of measuring the rheological properties of fluids. The operating principle of the device is to disturb the flow by bending the post in an oscillatory fashion with an electromagnet and recording the motion of the post with a microscope camera (Fig. 1). The response of the post behaves as a first order system with a modified spring constant and drag coefficient which relate directly to the Young's modulus and viscosity of the fluid.

II. Materials and Methods

A. Device Fabrication

Devices were fabricated using replica molding in an aluminum mold. Aluminum molds were made by drilling 250 μm through-holes in a 2.8 mm thick aluminum block. PDMS (Dow Corning, Sylgard 184) was made in a ratio of 10:1 base-to-crosslinker by mass. This mixture was then further mixed with iron microparticles (Sigma-Aldrich, 44890) in a ratio of 2:1 PDMS to iron by weight. After degassing, the PDMS-iron mixture was placed as a drop on a piece of foil, then the aluminum molds pushed against the drop to fill the mold. After filling the mold, it was placed on plain PDMS with a pre-cured PDMS backing. The purpose of this procedure was to keep the base of the mold transparent, and to prevent excess force on the post when a magnetic field was applied. The entire structure was then cured for 20 minutes at 110 °C, then the tops were sheared away with a razor blade, and the mold was pealed from the base (Fig. 2). Some holes were clogged during the peeling process, resulting in partially-formed posts which were discarded. Posts were cut from each other with a razor blade to form single posts standing on a base of PDMS. Each post was then affixed to a P-35 petri dish using additional PDMS at the base. A cloning ring (Fisher, 14-512-79) was

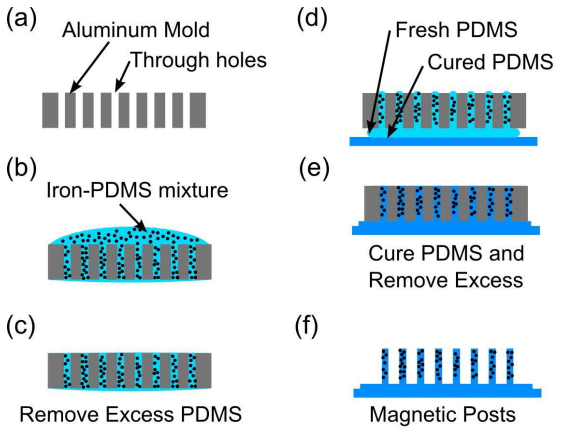

Fig. 2. Fabrication process for embedding particles in a microdevice. (a) Aluminum molds with through-holes are (b) filled with magnetically-doped PDMS. (c) Excess doped PDMS is removed, and (d) non-doped PDMS is used to affix it to a backing layer. (e) Posts are cured, and (f) the final posts are made with a length of 3.8 mm and diameter of 250 μm.

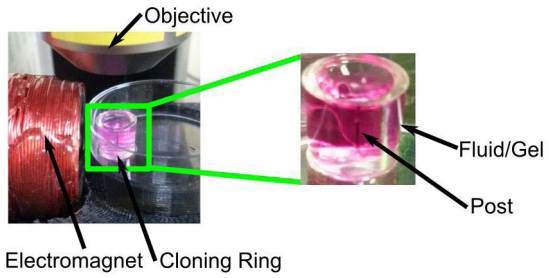

Fig. 3. Picture of the post filled with collagen gel under the microscope. A custom holder was manufactured to hold a petri dish in a position against an electromagnet. The entire structure was positioned on a microscope stage. Gels and fluids are contained in a cloning ring affixed to the petri dish.

then adhered to the dish with PDMS and located so the post was in the approximate center of the ring (Fig. 3).

B. Experimental Setup

Tests were run under a 10× objective on a microscope (Nikon, Eclipse NV100). A custom-built electromagnet was used to vary the magnetic field in a sinusoidal fashion. Images were taken at a rate of 45 frames/second using an Orca-Flash 2.8 camera (Hammamatsu, C11440-10C). The experimental setup was controlled with LabView. Regardless of the direction of the magnetic field, the post was pulled towards the magnet, and the total current running through the electromagnet was recorded using a DAQ (National Instruments, USB-6002). During each 5 second run, 200 images and the input voltages were recorded. Devices were calibrated with quasi-static runs where the current through the coil was oscillated at 0.25 Hz. The analysis runs were performed using a chirp signal. We have included four supplemental videos to show the post motion in collagen gels during a representative experiment. These videos will be available at http://ieeexplore.ieee.org.

The current to the electromagnet had a peak-to-peak amplitude of 1.5 A, which resulted in a peak-to-peak force of 2 μN. The field from the magnet varied from 23 to 25 mT throughout

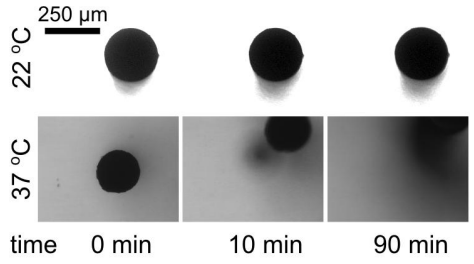

Fig. 4. Posts in collagen gels formed at 37 °C often had significant motion from the neutral position, while posts formed at 22 °C remained vertical. Experiments for viscoelasticity measurements were taken at 22 °C.

the length of the post, resulting in a load on the post that is less than 10%, as expected from modeling the electromagnet as a dipole [18]. Although the field is not uniform, we have made the assumption that the force is sufficiently uniform for our analysis, and this results in a load on the post determined by

$$F = BMV = (\mu_0 i)(\mu i) V \quad (1)$$

where F is the force on the post due to the magnetic field, B is the magnetic field generated by the coil, M is the induced magnetism of the iron particles, V is the volume of magnetic material in the post, μ_0 is the permeability of free space, μ is the permeability of iron, and i is the current in the coil [19]. As shown in (1) the force is dependent on the square of the current.

C. Fluid and Gel Preparation

Mixtures of glycerol (J. T. Baker, 2136-01) and water were used to calibrate the motion of the post in purely viscous fluids. Mixtures were prepared by mixing a volume ratio of 90%, 96.5%, and 100% glycerol in order to achieve a wide range of viscosities [20].

Collagen gels were formed with concentrations of 1 mg/mL or 3 mg/mL of collagen per standard protocols [21]. Stock rat tail collagen I with a concentration of 4.1 mg/mL (BD Bioscience, 354236) was diluted to form 1 mL of gel, with 10% volume of Medium 199 (Life Technologies, 11825-015). 1 N NaOH (Fisher, SS255-1) was added to the solution until it reached a pH of 7.1, which was indicated by a color change from yellow to pink. Water was added to the solution until to make up the remaining 1 mL volume. The solution was mixed throughly and pipetted into the wells. Gels which had trapped bubbles near the post were removed from analysis.

Collagen gels were initially formed at 37 °C, but there was concern about movement of the post while the solution underwent gelation, Fig. 4. In order to characterize the gelation process, posts were observed while they underwent gelation at either 37 °C or at room temperature (22 °C). As can be seen in Fig. 4, when gelling at an elevated temperature, the post moved significantly, whereas at room temperature, the post stayed relatively in the same position. After observing the significant motion of the post at 37 °C, rheology experiments with collagen gels were run at 22 °C. The post was actuated for four minutes at thirty minute intervals throughout

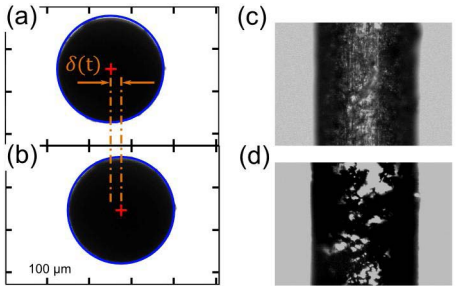

Fig. 5. Posts moved from an (a) actuated to an (b) unactuated position when the magnetic field is removed. A circular Hough fitting algorithm is used to determine the center of the posts in each image. Side views of magnetic posts with (c) reflective and (d) bright field show the density of microparticles.

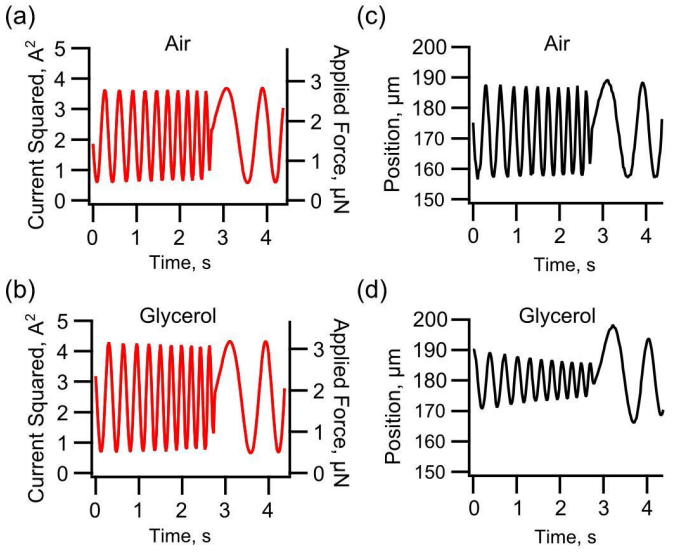

Fig. 6. Raw data traces of the (a) applied current and force compared with the resulting (b) position of the top of the post for air. The (c) applied force was the same for glycerol, while the (d) position response was reduced.

the experiment in order to determine the viscosity and elasticity of the fluid while it underwent the gelling process.

D. Image Analysis

Images were processed using a circular Hough fitting program in Matlab [22]. The centroid movement was tracked throughout the video and converted into micrometers. Typical images of the top of the post can be seen in Fig. 5. The voltage sent to the electromagnetic coil was measured and converted into current based on the resistance of the coil and the experimental setup. As previously mentioned, quasi-static experiments (0.25 Hz) were analyzed to determine a relationship between the square of the peak-to-peak current and the peak-to-peak position of the centroid. After calibrating the force relationship, parameters were determined using the System Identification Toolbox in Matlab. A first-order system was fit to the data and used to determine the constants in the system. Sample data for the input force and resulting position can be seen below in Fig. 6.

III. Device Theory

In order to characterize the dynamic motion of a post, we started with a simple first-order approximation of the

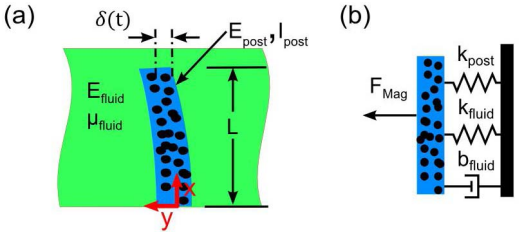

Fig. 7. (a) Interactions of the post with the fluid or gel result in a (b) free body diagram of the relevant parameters from a first order approximation of the system.

relationship between the applied force and the displacement of the top of the post

$$F(t) = \left(k_p + k_f\right)\delta(t) + \left(b_f\right)\dot{\delta}(t) \tag{2}$$

where $F(t)$ is the total distributed load on the post, $\delta(t)$ is the deflection of the top of the post, k_p is given by the elastic nature of the post, k_f is an experimentally determined coefficient relating to the elasticity of the fluid, and b_f is an experimentally determined coefficient relating to the damping in the system.

The loads on the post consist of the loading due to the magnetic force, the restoring force of the post as a cantilever, and the resistance on the post due to the fluid (Fig. 7). The magnetic force was assumed to be uniform throughout the post, and cross-sectional views of the post confirmed well-distributed particles throughout the post. The resistance of the fluid can be due to the viscosity of the fluid, or viscoelasticity of the gels. Our system involves tracking the top of the post instead of the entire length of the post and is operated at low frequencies. As others have done for magnetic beads [23], we assume that the effects due to the mass of the post are much less than the effects due to the stiffness and drag, which results in the first order approximation in (2).

A. Drag Forces

The drag force on the post is due to the fluid inside the cloning ring. The Reynold's number for our system is much less than one, which indicates that the viscous forces dominate over the inertial forces in the system. Stoke's flow around a bead can be used when the Reynold's number is much less than 1. In our system, there is a cylinder, and the analogous description of its drag force is given by the Oseen approximation [24]

$$\frac{F_{drag}}{L} = \frac{4\pi\mu}{\frac{1}{2} - \gamma - \ln\left(\frac{Re}{4}\right)}\frac{\partial y(t)}{\partial t} \tag{3}$$

where L is the length of the cylinder, μ is the viscosity of the fluid, $\partial y(t)/\partial t$ is the velocity of the cylinder, γ is Euler's constant, and Re is the Reynold's number.

The equation given in (3) assumes a uniform flow around a rigid cylinder, but our post is a cantilever bending into the fluid, so the velocity along its length is not constant. Thus, we approximate the flow around our cantilever by integrating (3) across the length of the cylinder to obtain

$$F_{drag} = \int_0^L \frac{4\pi\mu}{\frac{1}{2} - \gamma - \ln\left(\frac{Re}{4}\right)}\frac{\partial y(x,t)}{\partial t}dx. \tag{4}$$

The Reynold's number and viscosity can be approximated as constants with respect to x so the only parameter dependent on x is the velocity of the fluid, $\partial y\,(x,t)\,/\partial t$, which gives us

$$F_{drag} = \frac{4\pi\,\mu}{\frac{1}{2} - \gamma\, - \ln\left(\frac{Re}{4}\right)} \int_0^L \frac{\partial y\,(x,t)}{\partial t} dx. \tag{5}$$

Due to relatively small viscous forces compared with the elastic forces on the post, the shape of the post can be approximated as a cantilevered beam with a uniform load. Thus, the deflection of the top of the post is given by

$$y\,(x,t) = \delta\,(t)\,\frac{x^4 - 4x^3L + 6x^2L^2}{3L^4} \tag{6}$$

where $\delta(t)$ is the motion of the top of the post, and x is a position along the length of the post.

After combining (6) with (4) and integrating, we can determine a drag coefficient that can be used with the data from this experiment to determine the viscosity of the fluid interacting with the post

$$b_f = \frac{4\pi\,\mu}{\frac{1}{2} - \gamma\, - \ln\left(\frac{Re}{4}\right)} \frac{6}{15} L. \tag{7}$$

B. Elastic Forces

The restoring force on the post due to elastic forces, $k_f + k_p$, is due to the elasticity of the post, along with any elasticity from the viscoelastic fluid. Based on the geometry of the system, we can approximate the spring constant based on the relationship between displacement and force for a cantilevered beam with a uniformly distributed load supported on a Winkler foundation [25], where the gel in the well is the Winkler foundation material. The Winkler foundation is an infinite elastic half-space which is commonly used to model loads on foundations in engineered structures. There are exact solutions to numerous interactions between loading configurations and Winkler foundations, including one for an elastic beam interacting with the elastic foundation, which involves the modulus of both the beam and the modulus of the foundation

$$k_f + k_p = kL\left(1 - \frac{2\cosh\left(\lambda L\right)\cos\left(\lambda L\right)}{\cosh^2\left(\lambda L\right) + \cos^2\left(\lambda L\right)}\right) \tag{8}$$

where λ is given by $\lambda = \left(E_p/4kI\right)^{1/4}$, E_p is the Young's modulus of the PDMS post, k is the foundation modulus of the gel in the system, and I is the second moment of area of the post cross-section.

The foundation modulus, k, can be related to the Young's modulus, E_f, of the gel by assuming that the PDMS beam is relatively stiff compared with the gel, and that the gel interacts with a much stiffer base [26], [27]

$$E_f = \frac{\left(1 + \nu_f\right)\left(1 - 2\nu_f\right)}{\left(1 - \nu_f\right)} \frac{H}{b} k \tag{9}$$

where ν_f is the Poisson's ratio of the gel, H is the depth of the gel, and b is the width of the beam. In our system, we assume that Poisson's ratio of collagen is 0.25, although the exact value for collagen is unknown [28]. Slight variations in Poisson's ratio change the final stiffness calculation of the gels, but the stiffnesses are of the same order of magnitude. The modulus of PDMS and the modulus of polystyrene are both at least two orders of magnitude greater than the modulus of collagen, so the beam and base are both stiff compared to the gel.

The modulus of the PDMS-iron particle composite used in our analysis is 2.5 MPa. The modulus of PDMS with 6% volume iron particles was found to be 20-30% higher than that of plain PDMS through a tensile test, and that is consistent with previous results [29]. The exact modulus of PDMS, and PDMS with iron particles is highly dependent on many factors, including mixing ratio, baking time, baking temperature, storage time, and microparticle density [30].

In the event that the fluid in the ring is a purely viscous fluid, the portion of the spring constant due to the fluid will approach zero, and the material will behave as a Timoshenko beam [31]

$$EI\frac{\partial^4 y\,(x,t)}{\partial x^4} + m\frac{\partial^2 y\,(x,t)}{\partial t^2} = p\,(x,t) \tag{10}$$

where $y(x,t)$ is the total deflection of any point on the post, and it is determined based on the specific mass of the post, m, the Young's Modulus, E, the second moment of area, I, and the external loading on the post, $p(x,t)$. The magnetic forces on the beam are uniformly distributed across the length of the post, and the forces due to the mass of the beam are much smaller than those due to the elasticity of the beam. The solution to (10) can then be solved by using Castigliano's method [32] which relates the displacement of each point on an elastic structure to the strain energy in the structure. For a cantilevered beam with a circular cross-section and a uniformly distributed load, the solution is

$$k_p = \frac{E_p \pi\, d^4}{L^3} \tag{11}$$

where d is the diameter of the post, and L is the height of the post. This result is obtained as the modulus of the fluid, E_f, in (8) approaches zero.

C. Governing Equation and Material Properties

By combining our initial first order system (2) with the elastic forces (8) and the drag forces (7), we can put together a relationship between the applied magnetic force and the known and unknown parameters of the system

$$F_{mag}\,(t) = E_f L\left(1 - \frac{2\cosh\left(\lambda L\right)\cos\left(\lambda L\right)}{\cosh^2\left(\lambda L\right) + \cos^2\left(\lambda L\right)}\right)\delta\,(t) + \left(\frac{4\pi\,\mu}{\frac{1}{2} - \gamma\, - \ln\left(\frac{Re}{4}\right)}\right)\frac{6}{15} L\dot{\delta}\,(t)\,. \tag{12}$$

Comparing (2) and (13), the relationship between the experimentally determined damping coefficient, b_f, and the viscosity, μ, is given by

$$\frac{b_f}{\mu} = \frac{4\pi}{\frac{1}{2} - \gamma\, - \ln\left(\frac{Re}{4}\right)} \frac{6}{15} L. \tag{13}$$

The relationship between the spring constant in (12) and the fluid modulus is indirect, but can be calculated by solving (8)

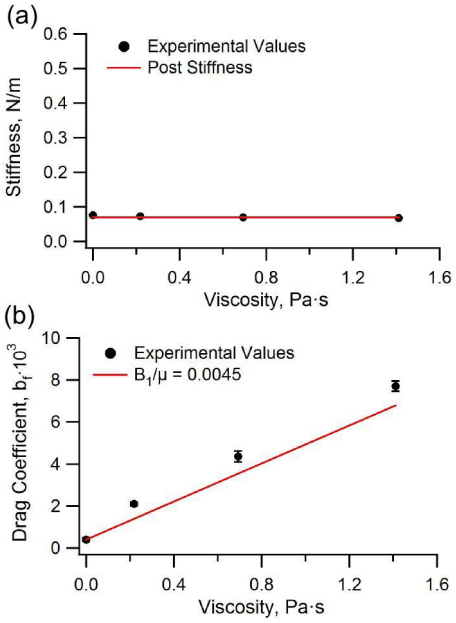

Fig. 8. Experimental results of the post response in glycerol mixtures. The (a) stiffness is equal to the post stiffness determined by (11), while the (b) relationship between drag and viscosity matches closely with the expected result from (13).

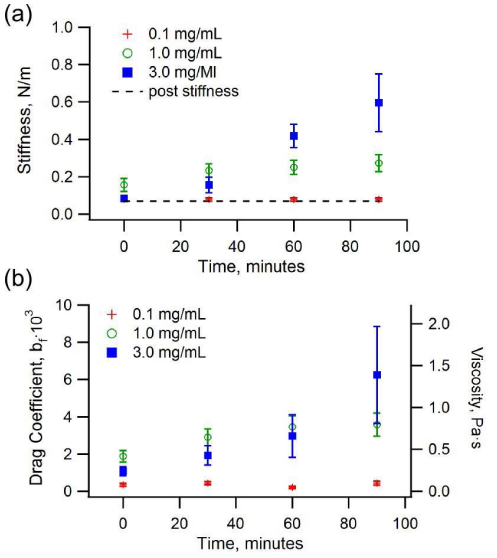

Fig. 9. Experimental results of the post response with different concentrations of collagen gels, showing the (a) stiffness coefficient and the (b) drag coefficient determined from the first order system. Experiments were run every 30 minutes during the gel formation.

for E_f. These two relationships can then give insight into how effective our new system is for determining material properties and outputting the results in commonly used parameters.

IV. Experimental Results

A. Viscous Fluids

In order to characterize the system, we first introduced purely viscous fluids in the form of mixtures of glycerol and air. As mentioned above, the stiffness of the post was governed by (11). The system was first calibrated at low frequencies in a quasi-static operation to set the ratio between the force and the square of the current, as given in (1). The results of the experiments can be seen in Fig. 8. The stiffness of the system was approximately equivalent to the expected stiffness of the post, which is due to the absence of any elastic component to glycerol mixtures. The experimentally-determined damping coefficient was linear, with a close approximation to the expected trend of 0.0045 $(\text{Pa}\cdot\text{s})^{-1}$.

B. Viscoelastic Gels

Collagen gels were observed over time and measured as they gelled. The stiffness and the damping coefficient were both determined over time and can be seen in Fig. 9. As expected, gels with a higher concentration of collagen ultimately had a higher elasticity and viscosity. In the case of the 1 mg/mL and 3 mg/mL gels, the elasticity and the viscosity both increased over time, while the 0.1 mg/mL gel behaved as a viscous fluid throughout the experiment.

As discussed above and shown in Eq. 8, the stiffness of the gel-post system can be used to determine the Young's modulus of the gel. There have been numerous studies on the modulus of collagen gels, including studies on the shear modulus [33], studies modeling gels to find the Young's modulus [34], [35], and studies on mixtures of gels with cells [36] or gluteraldehyde [37]. Data on the Young's modulus of gels varies between studies, primarily due to different methods of fabrication which affects the resulting modulus [33], although Roeder et al. [35] made gels similar to our technique, and gave a thorough analysis of the effects of pH, strain rate, and collage concentration on the modulus. The values found using our device are comparable to those of the Roeder study, Table I. Our values are generally lower, which may be due to a shorter gelation time.

TABLE I
Experimental Values for Collagen Gel Stiffness Compared to Previous Work

Concentration	Results (kPa)	Roder, et al. (kPa)
0.1 mg/mL	0.384 ± 0.2	
0.3 mg/mL		1.54 ± 0.507
1.0 mg/mL	3.792 ± 0.1	10.7 ± 1.93
3.0 mg/mL	9.360 ± 2.4	24.3 ± 4.16

V. Conclusion

We have successfully built and tested a novel rheology testing device which can be used to perform *in situ* testing of fluids and gels. We provided an analysis of how the system works and tested it against common fluids. In our device, fluids can be tested over time without causing destructive behavior to the fluids to determine how they behave. The device may also find applications in biology, where continuous monitoring of cell cultures over time can give an insight into the mechanical responses of tissues.

This device can only be used for relatively weak gels and fluids. The resolution of the position of the post does not

enable measurements of the viscoelasticity in regimes where the elasticity of the gel is high. This may be modified by applying a higher force to the post or increasing the amount of magnetic material in each post. Additionally, gels and fluids must be optically transparent or translucent in order to use the current system. Future systems may be able to make use of magnetic sensing techniques to eliminate this limitation.

One advantage of this device over current technologies is that it only requires small volumes in order to produce measurements of the bulk properties of the fluid or gel. Experiments in this paper were performed with 200 μL samples, and the volume can be further reduced by changing the size of the ring used to contain the fluid. This is particularly useful for situations where reagents are expensive.

The small size and biocompatibility of this device will make it useful for future studies with live cells or tissues *in situ* [38], [39]. The small size of the overall device makes is viable for studies which must be contained within an incubator which is useful for long-term culture or assessing cells on a continual basis. This device may be modified to provide parallel studies of many groups of cells. The device can be multiplexed and used for studying multiple interactions *in situ*.

ACKNOWLEDGMENT

The authors would like to thank Lilo Pozzo, Santosh Devasia, and Joseph Garbini for their help and useful suggestions.

REFERENCES

[1] A. R. Bausch, U. Hellerer, M. Essler, M. Aepfelbacher, and E. Sackmann, "Rapid stiffening of integrin receptor-actin linkages in endothelial cells stimulated with thrombin: A magnetic bead microrheology study," *Biophys. J.*, vol. 80, no. 6, pp. 2649–2657, 2001.

[2] J. Alcaraz *et al.*, "Microrheology of human lung epithelial cells measured by atomic force microscopy," *Biophys. J.*, vol. 84, no. 3, pp. 2071–2079, 2003.

[3] L. M. Rebêlo, J. S. de Sousa, J. M. Filho, J. Schäpe, H. Doschke, and M. Radmacher, "Microrheology of cells with magnetic force modulation atomic force microscopy," *Soft Matter*, vol. 10, no. 13, pp. 2141–2149, 2014.

[4] L. Chevry, N. K. Sampathkumar, A. Cebers, and J.-F. Berret, "Magnetic wire-based sensors for the microrheology of complex fluids," *Phys. Rev. E*, vol. 88, no. 6, p. 062306, 2013.

[5] P. Cicuta and A. M. Donald, "Microrheology: A review of the method and applications," *Soft Matter*, vol. 3, no. 12, pp. 1449–1455, 2007.

[6] L. G. Wilson and W. C. K. Poon, "Small-world rheology: An introduction to probe-based active microrheology," *Phys. Chem. Chem. Phys.*, vol. 13, no. 22, pp. 10617–10630, 2011.

[7] K. M. Schultz and E. M. Furst, "Microrheology of biomaterial hydrogelators," *Soft Matter*, vol. 8, no. 23, pp. 6198–6205, 2012.

[8] A. Magnin and J. M. Piau, "Cone-and-plate rheometry of yield stress fluids. Study of an aqueous gel," *J. Non-Newtonian Fluid Mech.*, vol. 36, pp. 85–108, Dec. 1990.

[9] B. A. Evans, A. R. Shields, R. L. Carroll, S. Washburn, M. R. Falvo, and R. Superfine, "Magnetically actuated nanorod arrays as biomimetic cilia," *Nano Lett.*, vol. 7, no. 5, pp. 1428–1434, 2007.

[10] A. R. Shields, B. L. Fiser, B. A. Evans, M. R. Falvo, S. Washburn, and R. Superfine, "Biomimetic cilia arrays generate simultaneous pumping and mixing regimes," *Proc. Nat. Acad. Sci. USA*, vol. 107, no. 36, pp. 15670–15675, 2010.

[11] F. Fahrni, M. W. J. Prins, and L. J. van Ijzendoorn, "Magnetization and actuation of polymeric microstructures with magnetic nanoparticles for application in microfluidics," *J. Magn. Magn. Mater.*, vol. 321, no. 12, pp. 1843–1850, 2009.

[12] F. Fahrni, M. W. J. Prins, and L. J. van Ijzendoorn, "Micro-fluidic actuation using magnetic artificial cilia," *Lab Chip*, vol. 9, no. 23, pp. 3413–3421, 2009.

[13] F. Khademolhosseini and M. Chiao, "Fabrication and patterning of magnetic polymer micropillar structures using a dry-nanoparticle embedding technique," *J. Microelectromech. Syst.*, vol. 22, no. 1, pp. 131–139, Feb. 2013.

[14] N. J. Sniadecki *et al.*, "Magnetic microposts as an approach to apply forces to living cells," *Proc. Nat. Acad. Sci. USA*, vol. 104, no. 37, pp. 14553–14558, 2007.

[15] J. le Digabel, N. Biais, J. Fresnais, J.-F. Berret, P. Hersen, and B. Ladoux, "Magnetic micropillars as a tool to govern substrate deformations," *Lab Chip*, vol. 11, no. 15, pp. 2630–2636, 2011.

[16] F. Tsumori and J. Brunne, "Magnetic actuator using interaction between micro magnetic elements," in *Proc. IEEE 24th Int. Conf. Micro Electro Mech. Syst. (MEMS)*, Jan. 2011, pp. 1245–1248.

[17] O. D. Oniku, B. J. Bowers, S. B. Shetye, N. Wang, and D. P. Arnold, "Permanent magnet microstructures using dry-pressed magnetic powders," *J. Micromech. Microeng.*, vol. 23, no. 7, p. 075027, 2013.

[18] J. M. D. Coey, *Magnetism and Magnetic Materials*. Cambridge, U.K.: Cambridge Univ. Press, 2010.

[19] D. Jiles, *Introduction to Magnetism and Magnetic Materials*. London, U.K.: Chapman & Hall, 1991.

[20] J. B. Segur and H. E. Oberstar, "Viscosity of glycerol and its aqueous solutions," *Ind. Eng. Chem.*, vol. 43, no. 9, pp. 2117–2120, 1951.

[21] (2014). *Collagen I, Rat Tail*. [Online]. Available: https://www.lifetechnologies.com/order/catalog/product/A1048301

[22] T. Peng, "Detect circles with various radii in grayscale image via hough transform," 2005. [Online]. Available: http://www.mathworks.com/matlabcentral/fileexchange/9168-detect-circles-with-various-radii-in-grayscale-image-via-hough-transform

[23] F. Ziemann, J. Rädler, and E. Sackmann, "Local measurements of viscoelastic moduli of entangled actin networks using an oscillating magnetic bead micro-rheometer," *Biophys. J.*, vol. 66, no. 6, pp. 2210–2216, 1994.

[24] W. P. Graebel, *Advanced Fluid Mechanics*. New York, NY, USA: Academic, 2007.

[25] M. Hetényi, *Beams on Elastic Foundation: Theory With Applications in the Fields of Civil and Mechanical Engineering*. Ann Arbor, MI, USA: Univ. Michigan Press, 1946.

[26] S. Krenk, *Mechanics and Analysis of Beams, Columns and Cables: A Modern Introduction to the Classic Theories*. Berlin, Germany: Springer-Verlag, 2001.

[27] K.-H. Chung, K. Bhadriraju, T. A. Spurlin, R. F. Cook, and A. L. Plant, "Nanomechanical properties of thin films of type I collagen fibrils," *Langmuir*, vol. 26, no. 5, pp. 3629–3636, 2010.

[28] D. M. Knapp, V. H. Barocas, A. G. Moon, K. Yoo, L. R. Petzold, and R. T. Tranquillo, "Rheology of reconstituted type I collagen gel in confined compression," *J. Rheol.*, vol. 41, no. 5, pp. 971–993, 1997.

[29] Z. Varga, G. Filipcsei, and M. Zrínyi, "Magnetic field sensitive functional elastomers with tuneable elastic modulus," *Polymer*, vol. 47, no. 1, pp. 227–233, Jan. 2006.

[30] D. Fuard, T. Tzvetkova-Chevolleau, S. Decossas, P. Tracqui, and P. Schiavone, "Optimization of poly-di-methyl-siloxane (PDMS) substrates for studying cellular adhesion and motility," *Microelectron. Eng.*, vol. 85, nos. 5–6, pp. 1289–1293, May 2008.

[31] H. Benaroya, *Mechanical Vibration: Analysis, Uncertainties, and Control*. Upper Saddle River, NJ, USA: Prentice-Hall, 1998.

[32] E. J. Hearn, *Mechanics of Materials: An Introduction to the Mechanics of Elastic and Plastic Deformation of Solids and Structural Materials*, vol. 1, 3rd ed. London, U.K.: Butterworth, 1997.

[33] Y.-L. Yang, L. M. Leone, and L. J. Kaufman, "Elastic moduli of collagen gels can be predicted from two-dimensional confocal microscopy," *Biophys. J.*, vol. 97, no. 7, pp. 2051–2060, 2009.

[34] A. M. Stein, D. A. Vader, D. A. Weitz, and L. M. Sander, "The micromechanics of three-dimensional collagen-I gels," *Complexity*, vol. 16, no. 4, pp. 22–28, 2011.

[35] B. A. Roeder, K. Kokini, J. E. Sturgis, J. P. Robinson, and S. L. Voytik-Harbin, "Tensile mechanical properties of three-dimensional type I collagen extracellular matrices with varied microstructure," *J. Biomech. Eng.*, vol. 124, no. 2, pp. 214–222, 2002.

[36] M. C. Evans and V. H. Barocas, "The modulus of fibroblast-populated collagen gels is not determined by final collagen and cell concentration: Experiments and an inclusion-based model," *J. Biomech. Eng.*, vol. 131, no. 10, pp. 101014-1–101014-7, 2009.

[37] M.-T. Sheu, J.-C. Huang, G.-C. Yeh, and H.-O. Ho, "Characterization of collagen gel solutions and collagen matrices for cell culture," *Biomaterials*, vol. 22, no. 13, pp. 1713–1719, 2001.

[38] S. L. Peterson, A. McDonald, P. L. Gourley, and D. Y. Sasaki, "Poly(dimethylsiloxane) thin films as biocompatible coatings for microfluidic devices: Cell culture and flow studies with glial cells," *J. Biomed. Mater. Res. A*, vol. 72A, no. 1, pp. 10–18, 2005.

[39] A. Folch and M. Toner, "Cellular micropatterns on biocompatible materials," *Biotechnol. Prog.*, vol. 14, no. 3, pp. 388–392, 1998.

Kevin S. Bielawski received the B.S.E. and M.S.E. degrees in mechanical engineering from the University of Michigan, Ann Arbor, in 2007 and 2008, respectively. He is currently pursuing the Ph.D. degree in mechanical engineering with the University of Washington, Seattle, as an ARCS Fellow. His research focuses on new devices for cell biomechanics.

Nathan J. Sniadecki received the B.S. degree from the University of Notre Dame, in 2000, and the M.S. and Ph.D. degrees from the University of Maryland, College Park, in 2003, under the supervision of Prof. D. DeVoe, all in mechanical engineering.

He was an NIH NRSA Postdoctoral Fellow in Biomedical Engineering with Johns Hopkins University and a Hartwell Fellow with the University of Pennsylvania in Bioengineering with Prof. C. Chen from 2004 to 2007. He joined as a Faculty Member with the University of Washington in 2007, where he is currently an Associate Professor with the Department of Mechanical Engineering and an Adjunct Associate Professor with the Department of Bioengineering. His work is on cell mechanics, mechanotransduction, and BioMEMS devices. He was a recipient of the NSF CAREER Award in 2009, a DARPA Young Faculty Award in 2011, and the Albert Kobayashi Professorship in 2012.